

## Evidence of C–H···O Hydrogen Bonds in Liquid 4-Ethoxybenzaldehyde by NMR and Vibrational Spectroscopies

M. P. M. Marques,<sup>†</sup> A. M. Amorim da Costa,<sup>†</sup> and Paulo J. A. Ribeiro-Claro<sup>\*,†,‡</sup>

Unidade Química-Física Molecular, Faculdade de Ciências e Tecnologia, Universidade de Coimbra, P-3004-353 Coimbra, Portugal, and Departamento de Química, Universidade de Aveiro, P-3810-193 Aveiro, Portugal

Received: December 31, 2000

Raman, FTIR, and NMR (both <sup>13</sup>C and <sup>17</sup>O) spectroscopies are used in a complementary way in order to study the occurrence of C–H···O intermolecular hydrogen bonds in liquid 4-ethoxybenzaldehyde (4EtOB). Additional information concerning the structure of the possible dimers is obtained through ab initio calculations, at the B3LYP/6-31G\* level. The strongest evidences of the presence of C–H···O hydrogen bonds in the liquid phase arise from the temperature and solvent intensity dependence of the two bands observed in the  $\nu_{\text{C=O}}$  region of the vibrational spectra, as well as from the shift to low magnetic field detected for the carbonyl <sup>17</sup>O NMR peak at higher dilutions. Further evidence is gathered from the changes observed in the  $\nu_{\text{C-H}}$  vibrational modes, the <sup>1</sup>J<sub>CH</sub> concentration dependence detected in the NMR spectra, and ab initio results. The experimental observations are consistent with the decrease of the C–H bond length upon hydrogen-bonding, as predicted for the nonstandard blue-shifting hydrogen bonds. Ab initio calculations predict several possible structures for the dimeric species, with nearly identical energies. The calculated dimerization energy is within the –5.1 to –6.5 kJ mol<sup>–1</sup> range, considering both basis set superposition error and zero-point vibrational energy corrections, in agreement with the obtained experimental  $\Delta H$  value of  $-5.7 \pm 0.5$  kJ mol<sup>–1</sup>.

### Introduction

It is nowadays well established that C–H···O close contacts play an important role in a wide variety of chemical phenomena, from crystal packing and molecular conformations to supramolecular design.<sup>1–5</sup> More exciting is the evidence that has been accumulated in the past decade, showing that this particular kind of interactions is of the utmost importance in the structure–activity relationships of biological systems.<sup>6–8</sup> The occurrence of C–H···O hydrogen bonds in the active sites of enzymes such as serine hydrolases<sup>7</sup> and their contribution to the helicoidal structure of RNA molecules<sup>8</sup> are two relevant examples. However, as most of the studies reported to date have been performed on crystal structures, based on both X-ray and neutron diffraction data, information on the role of this type of interaction in the liquid phase is still scarce. Recently, the presence of C–H···O bonded dimers in liquids has been inferred from both experimental and theoretical results for several hydroxyl- and carbonyl-containing molecules. In particular, Jedlosvszky and Turi used a Monte Carlo simulation,<sup>3</sup> based on previous ab initio results,<sup>9</sup> to conclude on the importance of C–H···O hydrogen bonds in liquid acetic acid. By comparing the infrared spectra of gaseous and liquid methanol, Yukhnevich and Tarakanova assigned particular spectral features to the formation of C–H···O bonds in the liquid phase.<sup>10</sup> Gil et al. combined ab initio results and Raman spectra of liquid samples in order to assess the effects of intramolecular C–H···O interactions on the conformational preferences of alkoxyethanol derivatives.<sup>11</sup>

Benzaldehyde derivatives are among the most interesting carbonyl-containing systems. In benzaldehyde itself, C–H···O close contacts have only been identified in crystalline inclusion compounds,<sup>12</sup> but spectroscopic evidence of these hydrogen bonds in the liquid phase has been found for some of its derivatives.<sup>13–15</sup> In particular, for 4-methoxybenzaldehyde, the presence of a dimerization equilibrium, with  $\Delta H = -7.6 \pm 0.9$  kJ mol<sup>–1</sup>, has been detected from both temperature variation Raman studies<sup>13</sup> and <sup>17</sup>O NMR spectra.<sup>14</sup> In turn, in 2-methoxybenzaldehyde the vibrational data suggest the presence of C–H···O bonded dimers in the liquid phase while a specific intermolecular CH···O contact has been identified in the solid by X-ray crystallography.<sup>15</sup>

In the present work, the study of C–H···O interactions in the liquid phase is performed for 4-ethoxybenzaldehyde (4EtOB; see Figure 1). Both <sup>13</sup>C and <sup>17</sup>O NMR, as well as FTIR and Raman, spectra are reported and discussed. Particular attention is given to the carbonyl stretching mode ( $\nu_{\text{C=O}}$ ) and to the carbonyl <sup>17</sup>O NMR chemical shift, which have been previously proved to be useful probes of hydrogen bonding to the carbonyl oxygen atom.<sup>14,16–20</sup> The nature of the C–H donors is evaluated from both the analysis of the  $\nu_{\text{C-H}}$  stretching region and the <sup>13</sup>C NMR pattern. To obtain additional information concerning the structure of the dimeric species, ab initio calculations, at the B3LYP/6-31G\* level, were performed for a set of most relevant interaction geometries.

### Experimental Section

Both 4-ethoxybenzaldehyde and the solvents used were of analytical grade (obtained from Sigma-Aldrich) and used without further purification.

The NMR spectra were run on a Varian Unity-500 Fourier transform spectrometer (operating at external magnetic fields

\* To whom correspondence should be addressed. Phone: +351-234370729. Fax: +351-234370084. E-mail: pclaro@ua.pt.

<sup>†</sup> Universidade de Coimbra.

<sup>‡</sup> Universidade de Aveiro.

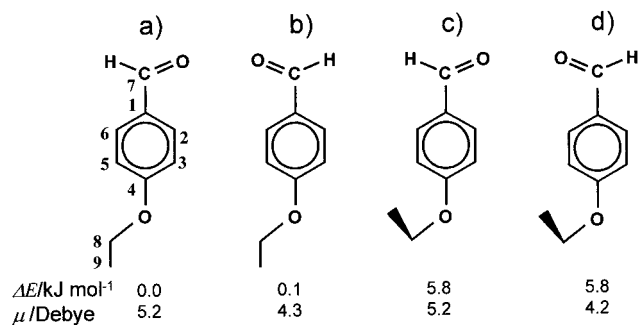


**Figure 1.** Chemical structure of 4EtOB, showing the atom numbering and the possible conformers (a–d). The relative energies and dipole moments of the conformers were computed at the B3LYP/6-31G\* level (see text). The absolute energy of conformer (a) is  $-499.4181263$  hartree/molecule.

of 2.97 and 1.60 T respectively for  $^{13}C$  and  $^{17}O$ ), in a 5 mm broad-band probe, at 298 K. For the  $^{13}C$  NMR experiments, recorded without proton-decoupling, the  $CCl_4$  peak was used as an internal reference ( $\delta = 96.7$  ppm). The  $^{17}O$  NMR spectra were obtained with  $D_2O$  as an external reference ( $\delta = 0$  ppm). Typically, spectral widths of 20 000 Hz, acquisition times of 0.4 s, pulse delays of 8–12 s, and ca.  $5 \times 10^3$  transients were used when obtaining  $^{13}C$  data. For  $^{17}O$  spectra (recorded with a standard Cyclops pulse sequence) the corresponding parameters were 50 000 Hz, 60 ms, 0.032 ms ( $90^\circ$ ), and  $6 \times 10^5$ . The  $^{17}O$  chemical shifts obtained are accurate up to  $\pm 1$  and  $\pm 3$  ppm for carbonyl and ethoxy oxygen atoms, respectively.

Raman spectra were recorded on a triple monochromator (Jobin Yvon T 64000) using a CCD (Jobin Yvon Spectraview 2D) detector. The liquid samples were sealed in Kimax glass capillaries (i.d. 0.8 mm). The sample was illuminated by the 514.5 nm line of an  $Ar^+$  laser (Coherent-Inova 90) with 50 mW at the sample position. The entry slit of the spectrometer was set to 200  $\mu m$ , while the slit between premonochromator and spectrograph was opened to 14 mm, yielding a resolution of approximately 3  $cm^{-1}$ . The error in wavenumber is estimated to be smaller than 1  $cm^{-1}$ .

The infrared spectra were recorded in the 400–4000  $cm^{-1}$  region, on a Mattson 7000 FTIR spectrometer, using a global source, a DTGS detector, and potassium bromide cells. The spectra were collected in 32 scans with a resolution of ca. 1  $cm^{-1}$ .

Ab initio calculations were performed using the Gaussian 98 program package,<sup>21</sup> running on a personal computer. Molecular structures of monomer and dimers were fully optimized at the B3LYP/6-31G\* level of calculation.<sup>22–24</sup> Harmonic vibrational wavenumbers were calculated at the same level, using analytic second derivatives, to confirm the convergence to minima on the potential energy surface and to evaluate the zero-point vibrational energies (ZPVE). The calculated wavenumbers were always scaled by a factor of 0.95, which provides the best fit with the experimental values. The basis set superposition error (BSSE) correction for the dimerization energies has been estimated by counterpoise (CP) calculations, using the MAS-SAGE option of Gaussian 98.

## Results and Discussion

**Vibrational Spectra.** The Raman and FTIR spectra of 4EtOB, in the 1650–1750  $cm^{-1}$ , region are shown in Figure 2. Previous assignment of the 4EtOB vibrational spectra relates the 1700  $cm^{-1}$  IR and the 1690  $cm^{-1}$  Raman bands to the  $\nu_{C=O}$  mode,<sup>25</sup> but no mention is made to the presence of the pair of bands now detected in both spectra. The similarity with the

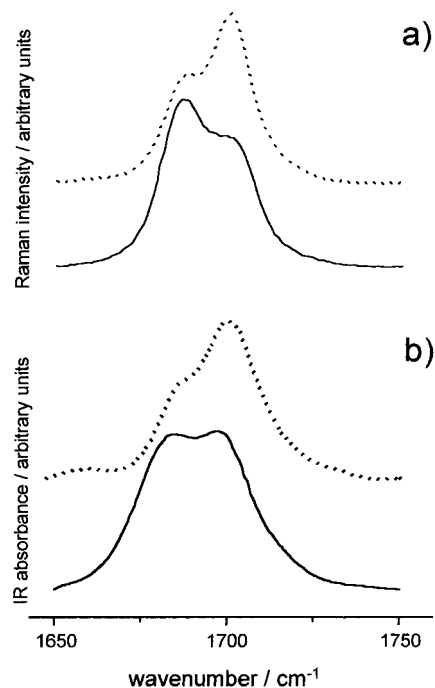


**Figure 2.** Room-temperature Raman (a) and FTIR (b) spectra of pure (solid line) and diluted 4EtOB ( $x = 0.1$  in  $CCl_4$ , dashed line) in the region of the C=O stretching modes.

results previously obtained for 4-methoxybenzaldehyde<sup>14</sup> suggests the assignment of the higher wavenumber component (1700  $cm^{-1}$ ) to the free C=O group and the lower wavenumber component (1690  $cm^{-1}$ ) to the hydrogen-bonded C=O group. However, two other possible causes for the band splitting, namely, Fermi resonance and conformational equilibrium, must be also considered and are presently discussed.

For several benzaldehyde derivatives, the presence of double bands in the  $\nu_{C=O}$  region has been ascribed to Fermi resonance between the  $\nu_{C=O}$  mode and presumably the first overtone of the out-of-plane (O=C–H) bending mode.<sup>26</sup> In 4EtOB, however, the observed intensity changes, either upon dilution or temperature variation—shown in Figures 2 and 3, respectively—do not support this assignment. In fact, the relative intensities of a Fermi dyad are not expected to change so drastically without significant shifts in the corresponding wavenumbers.

The 4EtOB molecule presents distinct conformers, schematically shown in Figure 1 (with their relative energies and dipole moments, calculated at the B3LYP/6-31G\* level). Both the C=O and O–C(8) bonds lie in the plane of the aromatic ring, and hence, two relative orientations are possible (hereafter named cis and trans, for simplicity). In addition, the ethyl group can adopt either anti or gauche orientations relative to the C(4)–O bond.

The  $\nu_{C=O}$  mode may be sensitive to either the cis/trans or (less probably) to the anti/gauche conformational equilibria, which would in either case lead to the presence of multiple bands in the  $\nu_{C=O}$  region. However, it was verified that dilution always causes an intensity increase of the 1700  $cm^{-1}$  band (Figure 2), regardless of the solvent polarity (e.g.,  $CCl_4$ ,  $\epsilon = 2.0$ , and  $CH_3CN$ ,  $\epsilon = 36.0$ ). Such an effect is not compatible with a conformational selection based on the dipole moment of the conformers. Moreover, the 1690  $cm^{-1}$  band displays an intensity increase only upon dilution with hydrogen-bond donor solvents (such as methanol), supporting its assignment to a hydrogen-bonded C=O group.

Thus, the presence of C–H···O hydrogen bonded dimeric species in liquid 4EtOB is the most reasonable explanation for

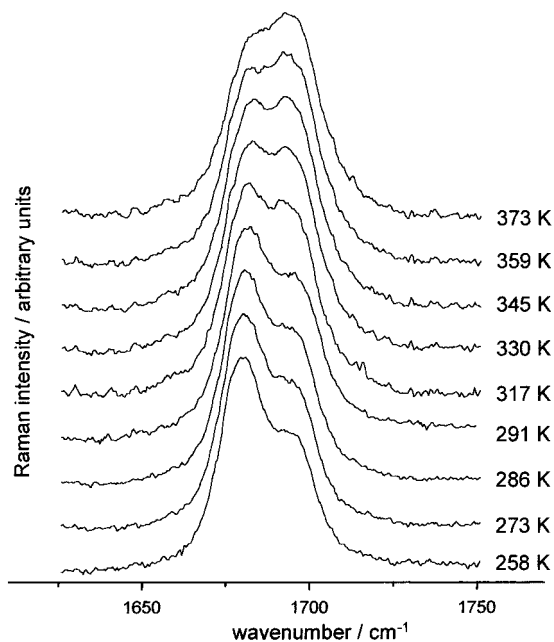


**Figure 3.** Raman spectra of pure 4EtOB at several temperatures, in the region of the C=O stretching modes.

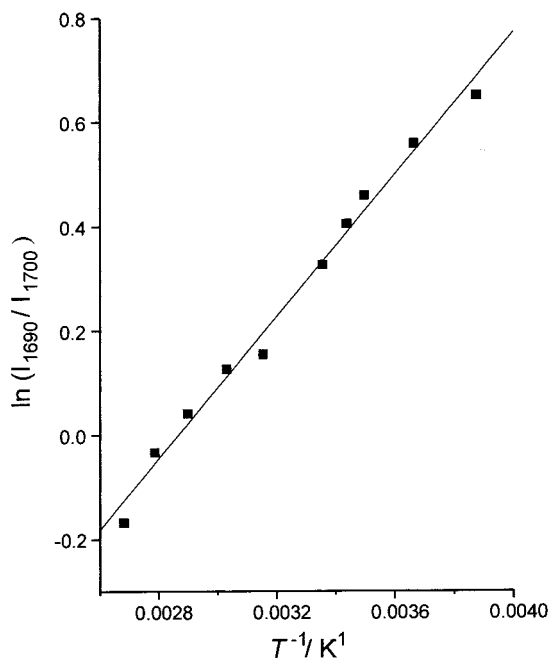


**Figure 4.** Plot of the logarithm of intensity ratio vs reciprocal temperature for the 1690/1700  $\text{cm}^{-1}$  band pair.

the observed spectral features in the  $\nu_{\text{C}=\text{O}}$  vibrational region. As shown in Figure 2, sample dilution leads to an increase of the free (monomer)  $\nu_{\text{C}=\text{O}}$  band intensity relative to the bonded (dimer)  $\nu_{\text{C}=\text{O}}$  band. Similarly, the intensity changes observed upon temperature variation follow the decrease of the dimer/monomer ratio with increasing temperature (Figure 3). A graphical logarithmic representation of the 1700/1690  $\text{cm}^{-1}$  intensity ratio vs the reciprocal temperature (Figure 4) yields a value of  $5.7 \pm 0.5 \text{ kJ mol}^{-1}$  for  $\Delta H$ . This value is within the range of the reported values for C-H $\cdots$ O dimerization equilibria.<sup>27</sup>

Additional information can be searched for in the spectral region comprising the  $\nu_{\text{CH}}$  vibrational modes. Figure 5 compares the Raman spectra of pure and diluted ( $x = 0.01$ ) 4EtOB, in the 2600–3200  $\text{cm}^{-1}$  range. This region can be roughly divided

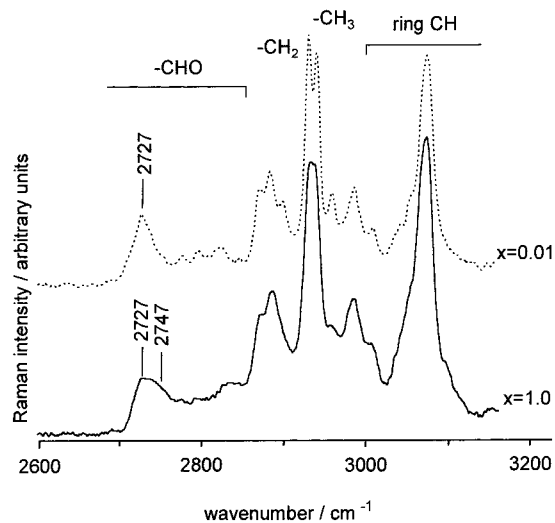


**Figure 5.** Room-temperature Raman spectra of pure (solid line) and diluted 4EtOB ( $x = 0.1$  in  $\text{CCl}_4$ , dashed line), in the region of the C-H stretching modes.

into three distinct zones, the aromatic (above 3000  $\text{cm}^{-1}$ ), the aldehydic (below 2850  $\text{cm}^{-1}$ , displaying several Fermi resonance components), and, between the two, the methyl and methylene  $\nu_{\text{CH}}$  modes. Comparison between the pure and diluted samples shows little intensity variations and wavenumber shifts, not easy to interpret. However, a significant change is observed for the strongest component of the aldehydic  $\nu_{\text{C}-\text{H}}$  mode (at ca. 2727  $\text{cm}^{-1}$ ). When the concentration of the sample gets higher, there is a clear intensity increase in the high wavenumber side of the 2727  $\text{cm}^{-1}$  band (at ca. 2742–2747  $\text{cm}^{-1}$ , Figure 5). In the FTIR spectra, this intensity increase leads to a blue shift of the absorption maximum (ca. 6  $\text{cm}^{-1}$ ) and an increase of the band half-width at half-height (ca. 3  $\text{cm}^{-1}$ ).

These observations can be directly related to the presence of C-H $\cdots$ O interactions. The broadening of the  $\nu_{\text{C}-\text{H}}$  band is expected upon C-H $\cdots$ O hydrogen bonding and has been reported for other systems.<sup>28</sup> On the other hand, a blue shift of the  $\nu_{\text{C}-\text{H}}$  mode has been predicted for C-H $\cdots$ O close contacts with weakly acidic C-H donors (being referred to as anti-hydrogen bonds<sup>29</sup> or improper blue-shifting hydrogen bonds<sup>30</sup> due to that unconventional behavior). Thus, the spectral changes illustrated in Figure 5 are in agreement with the participation of the aldehydic C-H bond in C-H $\cdots$ O interactions.

**NMR Spectra.** Figure 6 shows the concentration dependence of the  $^{17}\text{O}$  NMR chemical shifts for different 4EtOB solutions in  $\text{CCl}_4$ , with mole fractions of 4EtOB ( $x$ ) ranging from 0.025 to 1.0. The carbonyl- $^{17}\text{O}$  chemical shift decreases from 552 ppm, at  $x = 0.025$ , to 540 ppm, in the pure liquid, while the ethoxy- $^{17}\text{O}$  chemical shift varies within the 91–95 ppm interval. The carbonyl- $^{17}\text{O}$  chemical shift of substituted benzaldehyde derivatives has been reported to move to higher field upon intra- or intermolecular hydrogen bonding.<sup>18–20</sup> In the case of 4-methoxybenzaldehyde, a 15 ppm shielding was previously observed for the carbonyl oxygen atom upon hydrogen bonding.<sup>14</sup> The 12 ppm shielding effect upon concentration increase now observed for 4EtOB (Figure 6) is then in good accordance with the results on the 4-methoxy analogue,<sup>14</sup> although suggesting a somewhat weaker interaction. Thus—and in addition to the previously discussed vibrational data—these NMR results are strong evidence of the engagement of the carbonyl group in C-H $\cdots$ O hydrogen bonds in liquid 4EtOB.

The concentration dependence of the ethoxy- $^{17}\text{O}$  chemical shift is not as straightforward. As in the case of the 4-methoxy

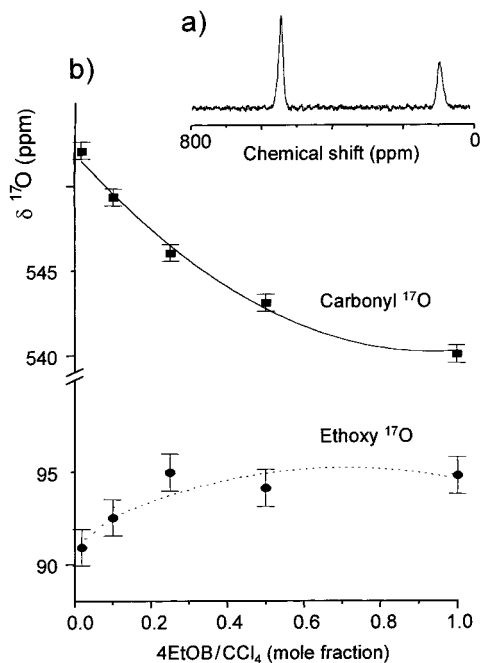


**Figure 6.**  $^{17}\text{O}$  NMR spectra of pure 4EtOB (a) and concentration dependence of the  $^{17}\text{O}$  chemical shift of several 4EtOB solutions in  $\text{CCl}_4$  (b): (■) carbonyl oxygen nucleus; (●) ethoxy oxygen nucleus. The dashed line across the ethoxy oxygen shifts is just meant as an eye guide.

analogue, two distinct effects, dominating the high- and low-concentration regions, appear to be present in 4EtOB. This may result from the combination of a bulk susceptibility effect and electron withdrawal by the hydrogen-bonded carbonyl group, but no further conclusions should be drawn from the present results alone.

It has been shown<sup>31,32</sup> that the proton-donating ability of a C–H bond can only be observed, by  $^1\text{H}$  NMR, when this interaction occurs with strong proton acceptors in sterically favorable circumstances. In such cases, the observed downfield shift is ca. 1–2 ppm<sup>32</sup> but becomes meaningless in the case of weaker interactions. In 4MeOB, for instance, the concentration dependence of this  $^1\text{H}$  NMR shift was found to be of the order of tenths of ppm, not allowing any definite conclusion regarding the presence of C–H···O hydrogen bonding.<sup>14</sup> On the other hand, several studies have focused on the relationship between C–H···X hydrogen bonding and C–H nuclear magnetic coupling (quantified by  $^1J_{\text{CH}}$  values).<sup>32–34</sup> It has been suggested that the increase of  $^1J_{\text{CH}}$  coupling for a C–H bond near either an F atom or a carbonyl oxygen gives evidence of the presence of a C–H···F or C–H···O hydrogen bond, respectively.<sup>32–34</sup> The observed increase ranges from ca. 10 Hz, in thiophene carbaldehydes ( $\text{O}=\text{C}-\text{H}\cdots\text{O}=\text{C}$  interaction),<sup>32</sup> to 3.7 Hz, in a triptycene derivative ( $\text{C}(\text{sp}^3)-\text{H}\cdots\text{F}$  interaction).<sup>34</sup> These values refer to intramolecular hydrogen bonding, much smaller values being expected for situations corresponding to higher motional freedom (and consequently shorter lifetimes for the C–H···X contacts), such as in intermolecular hydrogen bonding in liquids.

Figure 7 represents a plot of  $\Delta(^1J_{\text{CH}})$  as a function of concentration for the C(H) carbon atoms of 4EtOB in  $\text{CCl}_4$  solutions ( $\Delta$  values relative to the pure liquid). While  $^1J_{\text{CH}}$  for atom C(9) is nearly insensitive to dilution and the ring carbon  $^1J_{\text{CH}}$  values do not display a clear behavior,  $^1J_{\text{CH}}$  for C(7) and C(8) carbon atoms increases smoothly by ca. 1.7 and 0.8 Hz, respectively, from infinite dilution to the pure liquid.

In comparison with the above-reported values for the intramolecular C–H···O contacts, 1.7 Hz is rather significant.

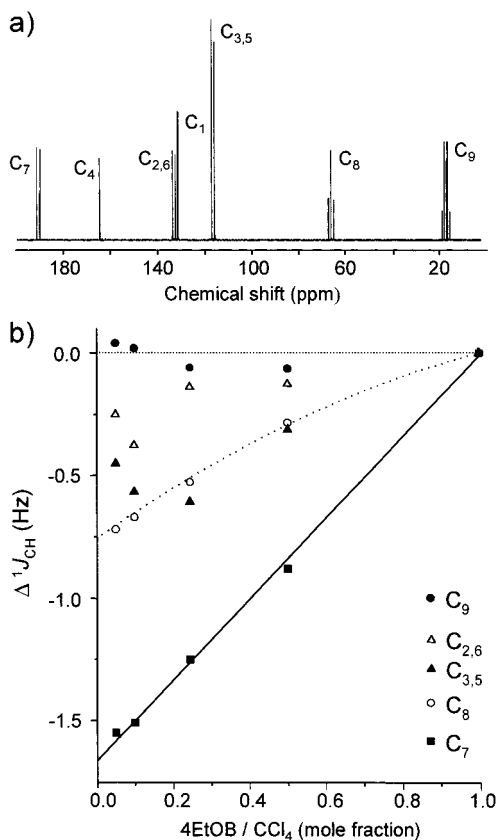


**Figure 7.**  $^{13}\text{C}$  NMR spectra of pure 4EtOB (a) and concentration dependence of the  $^1J_{\text{CH}}$  coupling constants of several 4EtOB solutions in  $\text{CCl}_4$  (b), relative to the pure liquid. The atoms are numbered according to Figure 1.

On the other hand, in the case of C(8), the observed  $^1J_{\text{CH}}$  is an average due to two protons, from which only one is expected to be engaged in hydrogen bonding at each time. Hence, both C(7) and C(8) display significant increases of the  $^1J_{\text{CH}}$  constant with concentration. This could suggest that the aldehydic C(7)–H and the methylene C(8)–H are the preferential donors in the C–H···O hydrogen bonds. Nevertheless, one must take into account that other effects are also most probably present. In particular,  $^1J_{\text{CH}}$  is known to increase with increasing electronegativity of the carbon atom substituents. In this way, the increase of the hydrogen bonding to the carbonyl oxygen atom (regardless of the donor) can also contribute to the observed increase of  $^1J_{\text{CH}}$  within the same formyl group.

**Ab initio Calculations.** Ab initio results are very useful in order to complement the spectroscopic information, particularly concerning the structure of the distinct dimeric species.

Figure 8 comprises the calculated optimized geometries (at the B3LYP/6-31G\* level) of the four most representative dimer structures, displaying more than a single C–H···O interaction. Although no systematic search of the configurational space was intended in this work, several other possible structures, namely, forms with single C–H···O contacts, C–H··· $\pi$  contacts, and stacking interactions of the aromatic rings, have been tested. According to the calculated energy differences, it is expected that the most significant dimer forms in the liquid phase arise from the four configurations in Figure 8. Naturally, several shorter lifetime forms are plausible to occur in the liquid, including forms with single C–H···O contacts and higher oligomers (trimers, tetramers, etc.).

In the representative set of Figure 8, the carbonyl oxygen atom is the preferential hydrogen bond acceptor, although

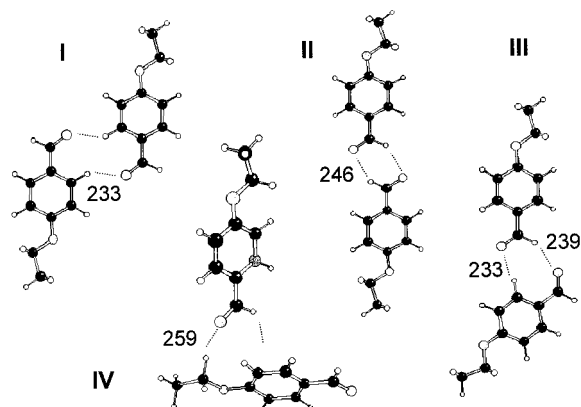


**Figure 8.** B3LYP/6-31G\* optimized geometries for four low-energy dimers of 4EtOB. Hydrogen bond distances are given in pm, the calculated dimerization energies for each dimer are listed in Table 1, and selected geometrical parameters and vibrational wavenumbers can be found in Table 2.

**TABLE 1: Dimerization Energies (Dimer–2 × Monomer) of 4EtOB<sup>a</sup> at the B3LYP/6-31G\* Level of Calculation**

energy corr	dimer ( $\Delta E/\text{kJ mol}^{-1}$ )			
	I	II	III	IV
none	-18.7	-16.9	-18.5	-17.4
ZPVE	-16.2	-14.3	-16.1	-15.2
CP	-8.2	-7.6	-9.0	-8.7
ZPVE+CP	-5.6	-5.1	-6.5	-6.5

<sup>a</sup> Absolute energy of structure I =  $-998.8433784E_h$ .

structure IV also presents a C–H $\cdots\pi$  contact. The ethoxy oxygen atom clearly displays lower acceptor ability. Regarding the C–H donors, the aldehydic C(7)–H and the ring C(2)–H will give rise to the stronger C–H $\cdots$ O bonds. Within the ethoxy group, only the methylene C(8)–H acts as a donor in energetically favored dimer structures. The strength of each contact can be evaluated through the C–H $\cdots$ O distance: the longest is observed for dimer IV (259 pm, methylene C–H donor) while the shortest occurs in dimers I and III (233 pm, ring C–H donor).

Table 1 contains the hydrogen bonding energies of the optimized dimers I–IV. The lowest energy minimum for the (4EtOB)<sub>2</sub> system depends on the level of correction considered, but all the dimeric species I–IV are less than 2 kJ mol<sup>-1</sup> apart. Since the product *RT* at 300 K is ca. 2.5 kJ mol<sup>-1</sup>, all of these structures can contribute to interactions in the liquid phase.

The uncorrected B3LYP dimerization energies are within the range of 16.9–18.7 kJ mol<sup>-1</sup>, while correction for both BSSE and ZPVE reduces these values to the 5.1–6.5 kJ mol<sup>-1</sup> range. The latter agrees well with the experimental  $\Delta H$  value of  $5.7 \pm 0.5$  kJ mol<sup>-1</sup>. Correction for both BSSE and ZPVE is expected to lead to overcorrected dimerization energies, as the ZPVE is not calculated for the BSSE corrected surface. However, according to a recent study,<sup>35</sup> the BSSE-corrected surface yields longer hydrogen-bond distances but not always a decrease in the ZPVE.

An interesting issue to be considered is the change in molecular structure associated with the dimerization process (Table 2). In fact, it was verified for 4EtOB that the C=O bond length increases from 121.8 pm, in the monomer, to over 122 pm, in dimers I–IV, as expected, due to the presence of a hydrogen bond. In turn, a different behavior is observed for the C–H bond lengths, which show a decrease when involved in a C–H $\cdots$ O interaction (the only exception being C(8)–H in dimer III). This calculated decrease of the C–H bond length

**TABLE 2: B3LYP/6-31G\* Bond Lengths (*l*) and Wavenumbers ( $\nu$ ) for the Monomer and Corresponding Bond Length Differences and Wavenumber Shifts (Relative to the Monomer) of the Dimeric Forms I–IV**

bond	monomer ( <i>l</i> /pm)	dimer ( $\Delta l$ /pm)			
		I	II	III	IV
C=O	121.8	0.3	0.6	0.3	0.6
C(7)–H	111.4	0.0	-0.6	-0.8	-0.1
C(8)–H	109.9	0.0	0.0	0.0	-0.3
C(2)–H	108.6	-0.1	0.0	0.1	-0.2

mode	monomer ( $\nu/\text{cm}^{-1}$ )	dimer ( $\Delta\nu/\text{cm}^{-1}$ )			
		I	II	III	IV
$\nu(\text{C}=\text{O})$	1700	-12	-35	-28	-22
		-8	-16	-7	-2
$\nu(\text{C}(7)\text{--H})$	2748	3	72	-1	-8
		4	78	101	29
$\nu(\text{C}(8)\text{--H}_2(\text{as}))$	2906	-2	-1	-3	30
$\nu(\text{C}(2)\text{--H})$	3045	9	-1	-8	-2
	3059	6	-1	-4	1

was previously reported for different molecular systems and is characteristic of C–H $\cdots$ O bonding with weak C–H donors.<sup>29,34,36–41</sup> Two experimental manifestations expected from the shortening of the C–H bond are the above-discussed increase of the <sup>1</sup>*J*<sub>CH</sub> coupling constant and the blue shift of the vibrational C–H stretching mode. Ab initio calculations predict wavenumber shifts in 4EtOB dimers I–IV of ca. 10, 30, and 80 cm<sup>-1</sup> for the ring, methylene, and aldehydic  $\nu_{\text{C–H}}$  modes, respectively. Actually, a blue shift of 71 cm<sup>-1</sup> was reported for an aldehydic  $\nu_{\text{C–H}}$  vibration in thiophene derivatives displaying intramolecular C–H $\cdots$ O bonding.<sup>32</sup> It is reasonable to expect that, in the case of intermolecular interactions, this kind of shift in wavenumber has a smaller magnitude. Calculated blue shifts reported for several halomethane derivatives with C–H $\cdots$ O<sup>38,41</sup> and C–H $\cdots\pi$ <sup>29,39,40</sup> intermolecular contacts are in the range of 12–55 cm<sup>-1</sup>, and the experimental value reported for the C–H $\cdots\pi$  interaction in the chloroform–fluorobenzene cluster<sup>40</sup> is 15 cm<sup>-1</sup>. As stated above, the observed blue shift for the aldehydic  $\nu_{\text{C–H}}$  mode in 4EtOB is within the range of 15–20 cm<sup>-1</sup>, when going from the diluted solution to the pure liquid.

As to the C=O bond length, the calculated increase upon hydrogen bonding (ca. 0.3–0.6 pm) is related to negative  $\nu_{\text{C=O}}$  frequency shifts, ranging from -7 to -35 cm<sup>-1</sup>. These calculated shifts are in reasonable agreement with the experimental value of -10 cm<sup>-1</sup>, considering that ab initio calculations refer to isolated species.

## Conclusions

The vibrational and NMR spectroscopic studies performed in the present work provide strong support for the presence of C–H $\cdots$ O bonded dimers in liquid 4EtOB. The strongest evidence arises from the temperature and solvent intensity dependence of the two bands observed in the  $\nu_{\text{C=O}}$  region, in both the Raman and FTIR spectra, as well as from the 12 ppm shift to higher field detected for the carbonyl-<sup>17</sup>O NMR chemical shift with increasing concentration. Further evidence is gathered from the changes in the  $\nu_{\text{C–H}}$  region, from the <sup>1</sup>*J*<sub>CH</sub> concentration dependence, and from ab initio calculations. In particular, the aldehydic C–H group displays an increase of both the  $\nu_{\text{C–H}}$  wavenumber and the <sup>1</sup>*J*<sub>CH</sub> coupling constant, from diluted solution to pure liquid. These experimental observations are consistent with the decrease of the C–H bond length upon hydrogen bonding, which as been predicted for the nonstandard blue-shifting hydrogen bonds.<sup>29,34,36–41</sup> These results are among

the first experimental evidences of the C–H bond length decrease upon C–H···O intermolecular hydrogen bonding.

Regarding the structure of the dimers, both the experimental and the computational results are consistent with the carbonyl oxygen atom being the hydrogen bond acceptor. The unambiguous assignment of the C–H donor, however, was not so straightforward. Although the  $^{13}\text{C}$  NMR results and the vibrational spectra in the  $\nu_{\text{C–H}}$  region can be interpreted as favoring the aldehydic C–H bond as the dominant hydrogen bond donor in the 4EtOB molecule, the possible participation of the methylene and ring C–H donors cannot be completely discarded.

Ab initio calculations predict several dimer structures with nearly identical energy. The calculated dimerization energy lies within the 5.1–6.5 kJ mol $^{-1}$  range after BSSE and ZPVE corrections, in agreement with the experimental  $\Delta H$  value of  $5.7 \pm 0.5$  kJ mol $^{-1}$ . It is interesting to note that both values (experimental and calculated) are ca. 2 kJ mol $^{-1}$  below the corresponding values for the 4-methoxy analogue.<sup>14</sup>

The decrease in the dimerization energy determined for 4-ethoxybenzaldehyde relative to the reported for the 4-methoxy derivative is in consonance with two other pieces of experimental evidence for the formation of C–H···O hydrogen bonds: when 4-ethoxy is compared to 4-methoxybenzaldehyde, the former displays a smaller split between the free and bonded  $\nu_{\text{C=O}}$  bands (10 vs 14 cm $^{-1}$ , respectively) and a smaller increase of the  $^{17}\text{O}$  NMR chemical shift upon dilution (12 vs 15 ppm). Since the ethoxy group has a lower electron donor character than the methoxy group, it is reasonable to conclude that the presence of electron donor substituents is important for the formation of C–H···O bonds in aldehydes, probably due to the increase of the electron density in the vicinity of the carbonyl oxygen atom.

The energy difference between the calculated dimer structures is below the  $RT$  value at room temperature; consequently, several dimeric species are expected to be present in the liquid phase. However, the energetic (enthalpic) factor is not the only one to be considered in the process of dimerization of 4EtOB, as the entropy change of the process is not independent of the structure of the dimer formed. In particular, and due to the presence of –CHO and –O–CH $_2$ –CH $_3$  internal rotations in the monomer, the entropic part of the C–H···O interaction must favor structure **II** (displaying total conformational freedom) relative to the other three dimeric forms (which have internal rotation restrictions). The same arguments should apply when considering the presence of forms with single C–H···O contacts (favored by entropy but not by enthalpy) and higher oligomers (favored by enthalpy but not by entropy).

## References and Notes

- (1) Desiraju, G. R. *Acc. Chem. Res.* **1996**, *29*, 441.
- (2) Steiner, Th. *Chem. Commun.* **1997**, 727.
- (3) Jedlovsky, P.; Turi, L. *J. Phys. Chem.* **1997**, *101*, 5429.
- (4) Ochsenbein, P.; Bonin, M.; Schenk, K.; Froidevaux, J.; Wytko, J.; Graf, E.; Weiss, J. *Eur. J. Inorg. Chem.* **1999**, *1999*, 1175.
- (5) Wahl, C. M.; Sundaralingam, M. *Trends Biochem. Sci.* **1997**, *22*, 97.
- (6) Marfurt, J.; Leumann, C. *Angew. Chem.* **1998**, *110*, 184; *Angew. Chem., Int. Ed. Engl.* **1998**, *37*, 175.
- (7) Derewenda, Z. S.; Derewenda, U.; Kobos, P. M. *J. Mol. Biol.* **1994**, *241*, 83.
- (8) Auffinger, P.; Westhof, E. *J. Mol. Biol.* **1997**, *274*, 54.
- (9) Turi, L. *J. Phys. Chem.* **1996**, *100*, 11285.
- (10) Yuhnevich, G. V.; Tarakanova, E. G. *J. Mol. Struct.* **1998**, *447*, 257.
- (11) Gil, F. P. S. C.; Amorim da Costa, A. M.; Teixeira-Dias, J. J. C. *J. Phys. Chem.* **1995**, *99*, 8066.
- (12) Harata, K.; Uekama, K.; Otagiri, M. *Bull. Chem. Soc. Jpn.* **1981**, *54*, 1954.
- (13) Ribeiro-Claro, P. J. A.; Batista de Carvalho, L. A. E.; Amado, A. M. *J. Raman Spectrosc.* **1997**, *28*, 867.
- (14) Karger, N.; Amorim da Costa, A. M.; Ribeiro-Claro, P. J. A. *J. Phys. Chem. A* **1999**, *103*, 8672.
- (15) 2-Methoxybenzaldehyde: the crystal structure is built up from an asymmetric unit of four molecules on the space group  $P4_3$ , presenting several C–H···O intermolecular contacts. The shortest one occurs between the carbonyl oxygen atom and the ring C(3)–H bond (poster presentation at the EUCCO-CC3, Budapest; manuscript in preparation).
- (16) Pimentel, G. C.; McClellan, A. L. *The Hydrogen Bond*; Freeman: San Francisco, CA, 1960; Chapter 3.
- (17) Amour, Th. E. St.; Burger, M. I.; Valentine, B.; Fiat, D. *J. Am. Chem. Soc.* **1981**, *103*, 1128.
- (18) Jaccard, G.; Lauterwein, J. *Helv. Chim. Acta* **1986**, *69*, 1469.
- (19) Boykin, D. W.; Chandrasekaran, S.; Baumstark, A. L. *Magn. Reson. Chem.* **1993**, *31*, 489.
- (20) Contreras, R. H.; Biekofsky, R. R.; Esteban, A. L.; Diez, E.; Fabian, J. S. *Magn. Reson. Chem.* **1996**, *34*, 447.
- (21) Frisch, M. J.; Trucks, G. W.; Schlegel, H. B.; Scuseria, G. E.; Robb, M. A.; Cheeseman, J. R.; Zakrzewski, V. G.; Montgomery, J. A.; Stratmann, R. E.; Burant, J. C.; Dapprich, S.; Millam, J. M.; Daniels, A. D.; Kudin, K. N.; Strain, M. C.; Farkas, O.; Tomasi, J.; Barone, V.; Cossi, M.; Cammi, R.; Mennucci, B.; Pomelli, C.; Adamo, C.; Clifford, S.; Ochterski, J.; Petersson, G. A.; Ayala, P. Y.; Cui, Q.; Morokuma, K.; Malick, D. K.; Rabuck, A. D.; Raghavachari, K.; Foresman, J. B.; Cioslowski, J.; Ortiz, J. V.; Stefanov, B. B.; Liu, G.; Liashenko, A.; Piskorz, P.; Komaromi, I.; Gomperts, R.; Martin, R. L.; Fox, D. J.; Keith, T.; Al-Laham, M. A.; Peng, C. Y.; Nanayakkara, A.; Gonzalez, C.; Challacombe, M.; Gill, P. M. W.; Johnson, B. G.; Chen, W.; Wong, M. W.; Andres, J. L.; Head-Gordon, M.; Replogle, E. S.; Pople, J. A. *Gaussian 98*, revision A.3; Gaussian Inc.: Pittsburgh, PA, 1998.
- (22) Lee, C.; Yang, W.; Parr, R. G. *Phys. Rev.* **1988**, *B37*, 785.
- (23) Becke, A. D. *J. Chem. Phys.* **1993**, *98*, 5648.
- (24) Hariharan, P. C.; Pople, J. A. *Theo. Chim. Acta* **1973**, *28*, 213.
- (25) Venkaji, P. *Spectrochim. Acta* **1986**, *42A*, 1301.
- (26) Nyquist, R. A. *Appl. Spectrosc.* **1992**, *46*, 306.
- (27) Goel, A.; Rao, C. N. R. *Faraday Trans.* **1971**, 2828.
- (28) de Matas, M.; Edwards, H. G. M.; Lawson, E. E.; Shields, L.; York, P. *J. Mol. Struct.* **1998**, *440*, 97.
- (29) Hobza, P.; Spirko, V.; Selze, H. L.; Schlag, E. W. *J. Phys. Chem. A* **1998**, *102*, 2501.
- (30) Muller-Dethlefs, K.; Hobza, P. *Chem. Rev.* **2000**, *100*, 143.
- (31) Nishio, M.; Hirota, M.; Umezawa, Y. *The CH $\pi$  Interaction: Evidence, Nature, and Consequences*, 1st ed.; Wiley-VCH: New York, 1998; Chapter 4.
- (32) Satonaka, H.; Abe, K.; Hirota, M. *Bull. Chem. Soc. Jpn.* **1988**, *61*, 2031.
- (33) Afonin, A. V.; Sigalov, M. V.; Korustova, S. E.; Aliev, I. A.; Vashchenko, A. V.; Trofimov, B. A. *Magn. Reson. Chem.* **1990**, *28*, 580.
- (34) Vizzioli, C.; de Azua, M. C. R.; Giribert, C. G.; Contreras, R. H.; Turi, L.; Dannenberg, J. J.; Rae, I. D.; Weigold, J. A.; Malagoli, M.; Zanasi, R.; Lazzaretti, P. *J. Phys. Chem.* **1994**, *98*, 8858.
- (35) Simon, S.; Duran, M.; Dannenberg, J. J. *J. Chem. Phys.* **1996**, *105*, 11024.
- (36) Turi, L.; Dannenberg, J. J. *J. Phys. Chem.* **1993**, *97*, 12197.
- (37) Gil, F. P. S. C.; Teixeira-Dias, J. J. C. *J. Mol. Struct. (THEOCHEM)* **1996**, *363*, 311.
- (38) Gu, Y.; Kar, T.; Scheiner, S. *J. Am. Chem. Soc.* **1999**, *121*, 9411.
- (39) Cubero, E.; Orozco, M.; Hobza, P.; Luque, F. J. *J. Phys. Chem A* **1999**, *103*, 6394.
- (40) Hobza, P.; Spirko, V.; Havlas, Z.; Buchhold, K.; Reimann, B.; Barth, H.-D.; Brutschy, B. *Chem. Phys. Lett.* **1999**, *299*, 180.
- (41) Hobza, P.; Havlas, Z. *Chem. Phys. Lett.* **1999**, *303*, 447.